Simultaneous Temperature and Refractive Index Measurements Using a 3° Slanted Multimode Fiber Bragg Grating

Chun-Liu Zhao, Xiufeng Yang, M. S. Demokan, *Senior Member, IEEE*, and W. Jin, *Senior Member, IEEE*

***Abstract*—A novel and simple sensor based on a 3° slanted multimode fiber Bragg grating (MFBG) for simultaneous temperature and refractive index measurement is demonstrated. The 3° slanted MFBG shows two wavelength groups in its transmission spectrum: One group, due to the coupling from one core mode to cladding modes, is sensitive to both surrounding refractive index (SRI) and temperature and the other, due to the coupling from one core mode to other core modes is sensitive only to temperature. Utilizing the obvious difference of two transmission dips in different wavelength groups on the temperature and the refractive index, two parameters can be distinguished and measured simultaneously using one slanted MFBG.**

***Index Terms*—Multimode fiber Bragg grating, sensor, simultaneous temperature and refractive index measurement.**

I. Introduction

OPTICAL sensors based on fiber gratings, including fiber Bragg gratings (FBGs) and long-period gratings (LPGs), have attracted much attention in recent years due to their wide applications in various physical parameter measurements such as strain, displacement, and temperature. LPGs have been utilized for refractive index and concentration sensing because the rejection bands that arise from light coupling from the fundamental mode to the forward-propagating cladding modes of the fiber are sensitive to the surrounding refractive index (SRI) [1]–[5]. However, because LPGs are also sensitive to temperature, the temperature effect must be distinguished or eliminated when they are used in refractive index sensing [2]–[4]. Furthermore, the temperature cross-sensitivity problem will cause an imprecise determination of the concentration since the refractive index of a chemical is a function of temperature. Thus, it is desirable to simultaneously measure temperature and SRI in these applications.

One suggestion for the simultaneous measurement of temperature and refractive index was by employing an additional FBG sensor as a temperature monitor cooperating with an LPG index sensor [1]. It was also proposed that two cascaded LPGs with different periods fabricated in a double-cladding fiber [3], as well as a sampled FBG [4], were used to achieve simultaneous temperature and refractive index measurement.

Besides LPGs, refractive index sensors based on FBGs have also been proposed. Most of them rely on the change of the evanescent field of the guided fiber mode with SRI by etching or side polishing FBGs [6]. This process could significantly weaken the FBGs. Laffont and Ferdinand utilized a tilted FBG in a single-mode fiber (SMF) to realize refractive index sensing, in which the losses due to coupling to the cladding modes at wavelengths below the Bragg wavelength were measured to deduce the change in SRI [7].

In this paper, we propose a novel and simple sensor based on a slanted multimode FBG (MFBG) for simultaneous temperature and refractive index measurement. Two different wavelength groups appear in the transmission spectra of a 3° slanted MFBG [8] since the couplings from one core mode to higher backward-propagating core modes and to cladding modes occur simultaneously. These transmission dips due to the coupling from one core mode to the cladding modes are sensitive to both SRI and temperature; meanwhile, the dips due to the coupling from one core mode to other core modes are sensitive to temperature only. Similar to the sensing principle reported in [3] and [4], temperature and SRI can be measured simultaneously by using only a 3° slanted MFBG, giving rise to a simpler and more compact sensor. One further advantage of this technique is that the bending effect on the 3° slanted MFBG can be ignored since FBGs with short periods are not sensitive to bending. Thus, this property of the sensor based on the MFBG provides a flexible and convenient measurement and avoids the requirement of a special V-groove plate in the sensors based on LPGs [1], [3]–[5]. Furthermore, the sharp transmission dips of Bragg gratings can prevent the reduction in the resolution caused by the relatively large rejection bandwidth of the sensors based on LPGs [5].

The remainder of the paper is constructed as follows. Section II describes the characteristics of a slanted MFBG. The operation principle is demonstrated for simultaneous temperature and refractive index measurement using a 3° slanted MFBG based on an understanding of the properties of core modes and cladding modes of a typical graded-index multimode fiber (MMF) in theory. Section III describes the experimental demonstration of simultaneous temperature and refractive index measurement using the 3° slanted MFBG. Experimental results are then compared with simulation results.

Manuscript received June 22, 2005; revised September 12, 2005.

C.-L. Zhao, M. S. Demokan, and W. Jin are with the Department of Electrical Engineering, The Hong Kong Polytechnic University, Hung Hom, Kowloon, Hong Kong (e-mail: eeclzhao@polyu.edu.hk).

X. Yang is with the Lightwave Department, Institute for Infocomm Research, Kent Ridge 637723, Singapore.

Digital Object Identifier 10.1109/JLT.2005.862471

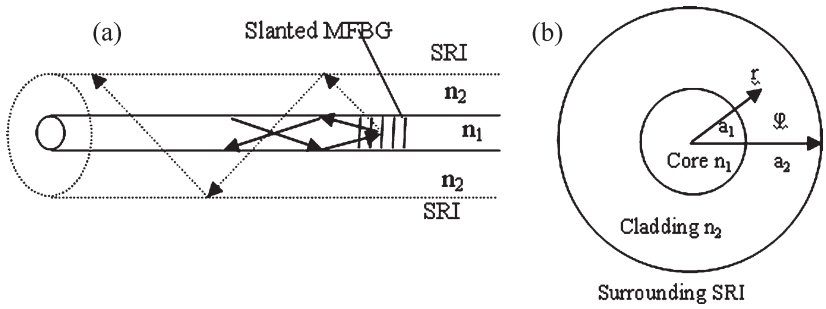

Fig. 1. (a) Schematic of the slanted MFBG. (b) Cross-sectional geometry of the MMF. The MFBG couples light from a core mode to other core modes (solid line) and cladding modes (dashed line).

II. Principle of Operation

Fig. 1 shows a schematic of a slanted FBG in a graded-index multimode fiber (MMF). We denote the highest refractive index of the fiber core as n_1, the refractive index of the fiber cladding as n_2, and the refractive index of the surrounding material as SRI. Because many modes can propagate simultaneously in the fiber core, a slanted MFBG may couple light from some core modes to other backward propagating core modes and/or cladding modes, according to phase matching conditions [8], [9]. The phase matching condition or Bragg reflection condition can be expressed as

$$\lambda = \frac{(n_i + n_j)\Lambda}{\cos(\theta)} \tag{1}$$

where λ is the wavelength, Λ and θ are the index modulation period and the slant angle of the MFBG, and n_i and n_j are the effective indexes of a forward propagating core mode and a backward propagating core (or cladding) mode. As mentioned in [8], the slant angle θ of the MFBG will largely affect the kinds of couplings occurring in the grating. When θ is between 2.5° and 4°, the couplings between core modes and other core modes, and those between core modes and cladding modes, will occur simultaneously. Here, we choose a 3° slanted MFBG for the objective of simultaneous temperature and refractive index measurements, and distinguish the wavelengths of transmission dips caused by coupling between core modes and other core modes by denoting them as $\lambda_{\rm co}$ and those caused by coupling between core modes and cladding modes as $\lambda_{\rm cl}$.

Many analyses show that some of the core modes in a graded-index MMF have almost the same propagation constant (effective index), and those modes having the same propagation constant form a mode group [8]–[13]. Here, we adopt the concept of principle mode as used in [8]–[10], that is, the core modes with the same propagation constant are classified into the same principal mode. According to the Wentzel–Kramers–Brillouin (WKB) method [11], the effective index for the Nth principal core mode can be expressed as

$$n_{\rm co}^N = n_1 \left[1 - \frac{\lambda\sqrt{2\Delta}}{\pi n_2 a_1}(N+1)\right]^{\frac{1}{2}} \tag{2}$$

where Δ is the maximum relative index difference of the MMF, a_1 is the radius of the core, and N is an integer. The parameters

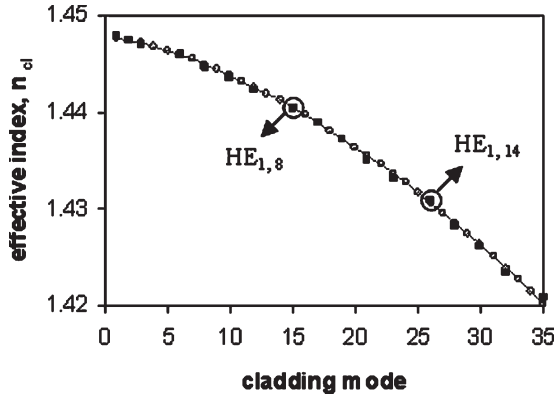

Fig. 2. Effective indices of cladding modes in the MMF when SRI = 1. ■: obtained from theory, modes of $HE_{1,v}$; ○: obtained from experiment.

of n_1, n_2, Δ, and a_1 are 1.4657, 1.448, 0.012, and 31.25 μm, respectively, for the MMF used in the experiment, which are obtained from the company supplying the fiber.

The effective indices of the core modes are determined only from n_1 and n_2 and are insensitive to SRI, as shown in (2). So the transmission dips $\lambda_{\rm co}$ do not change with a different refractive index of the surrounding material. In our experiment, the light propagating in the MMF before reaching the grating will be mainly the 0th principal mode because only a few modes are excited when the light source is coupled into the MMF. We can find that $n_{\rm co}^0$ is about 1.464 by substituting the relevant parameters of the fiber in (2).

The effective indices of the modes propagating in the cladding of the MMF are affected strongly by the SRI. An exact vector-field treatment must be used to obtain the cladding modes since the interface between the cladding and the fiber's surrounding medium might have a large refractive index difference. Here, we assume a simple three-layer step-index fiber geometry [as shown in Fig. 1(b)] and use the method demonstrated in [14] and [15] to get the effective indices of cladding modes $(HE_{l,v})$. Even though the fiber we used in the experiment is a graded-index fiber, we have assumed the fiber to be step-index in the computer simulation due to the simplicity in the modeling. By solving the dispersion relation for cladding modes with azimuthal dependence $\exp(\pm il\varphi)$ [14], the effective indices $(n_{\rm cl})$ of cladding modes are obtained such that SRI $< n_{\rm cl} < n_2$. Fig. 2 shows the effective indices of cladding modes with $l = 1$ (namely, $HE_{1,v}$) when SRI $= 1$ from theoretical consideration (squares), as well as

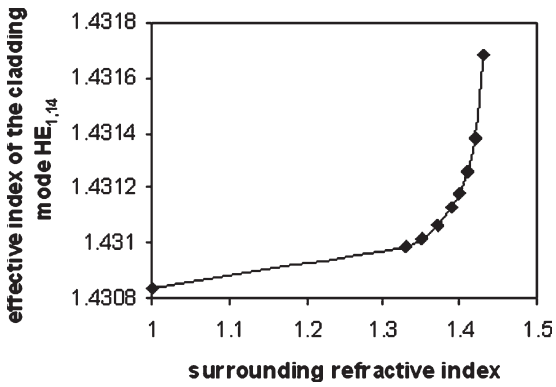

Fig. 3. Theoretical dependence of the effective index of $HE_{1,14}$ on the SRI.

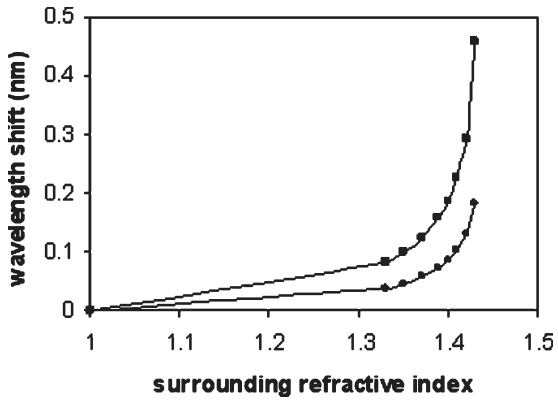

Fig. 4. Theoretical dependence of the wavelength shift with SRI for two transmission dips in the short wavelength range. ■: $\lambda_{\mathrm{cl},1} = 1556.03$ nm due to the core mode coupling to $HE_{1,14}$; •: $\lambda_{\mathrm{cl},2} = 1561.30$ nm due to the core mode coupling to $HE_{1,8}$.

the experimental values (circles) of the effective indices of these cladding modes coupled from the 0th principal core mode by the grating, which are obtained by substituting n_{co}^0 and transmission wavelengths λ_{cl} of the 3° slanted MFBG to (1). In Fig. 2, there are more circles (experiment) than squares (simulation) because the simulation results are only for $l = 1$, whereas the experimental results are for all modes. The results obtained from theory and experiment are in good agreement. In order to observe the effect of the SRI on cladding modes, we choose one cladding mode $HE_{1,14}$ as a sample and repeat the calculation for several SRI values. Fig. 3 shows the dependence of the effective index $(HE_{1,14})$ on SRI in theory. It is clear that the effective index increases rapidly with increasing SRI. This effect will lead to changes in the wavelengths reflected by the MFBG due to core modes coupling to cladding modes (λ_{cl}) as SRI changes. Here, we consider two kinds of mode couplings occurring in the 3° slanted grating: one is from the 0th principal core mode to the $HE_{1,14}$ cladding mode, and another is from the 0th principal core mode to the $HE_{1,8}$ cladding mode, respectively. Their resonant wavelengths (transmission dips) are about $\lambda_{\mathrm{cl},1} = 1556.03$ nm and about $\lambda_{\mathrm{cl},2} = 1561.30$ nm, obtained by the phase matching condition given by (1) when SRI $= 1$. The wavelength shifts with SRI can be obtained in theory by repeating the calculation for several SRIs as shown in Fig. 4. The resonant wavelengths of both mode couplings increase with increasing SRI. Particularly, the wavelength shift is larger for the coupling to $HE_{1,14}$ than that for the coupling to $HE_{1,8}$, since the higher-order cladding modes extend further into the surrounding medium. Besides this, the value of the wavelength shift is also affected by the slant angle of the MFBG. From (1), we can get that the wavelength shift caused by the effective index change of one cladding mode $\Delta\lambda$ equals $(n'_{\mathrm{cl}} - n_{\mathrm{cl}})\Lambda/\cos(\theta)$. Obviously, the wavelength shift is larger in the case of the MFBG with a large slant angle; thus, the sensor response is higher. Of course, the slant angle must be in the range of 2.5–4° because core to core mode couplings and core to cladding mode couplings can occur simultaneously in the MFBG for this range of slant angle [8].

From the analysis presented above, we conclude that λ_{co} is only sensitive to temperature and is not SRI dependent, while λ_{cl} is sensitive to both temperature and SRI. Therefore, the temperature can be measured from λ_{co} response and the SRI information can be measured exactly by extracting the temperature effect from the total response of the λ_{cl}. Furthermore, we have shown that if we choose the transmission dip due to a core mode coupling to a higher order cladding mode as a reference point for our measurement, we can obtain a better sensitivity to the changes in SRI.

III. Experiment and Results

In the experiment, a 3° slanted MFBG with 12-mm exposure length is fabricated in a hydrogen-loaded multimode fiber using phase mask illuminated directly by UV light. The fiber is a standard graded-index multimode fiber with a core diameter of 62.5 μm. The phase mask with a constant period of 1073.6 nm (the corresponding grating period is 536.8 nm) is placed on top of the fiber and paralleled to the fiber in close proximity. The slant angle of the MFBG is formed by adjusting the angle θ between the horizontal axial of the mask and the fiber. After writing, the slanted MFBG is then annealed at 120 °C for about 12 h to remove any unreacted hydrogen. The spectra of an MFBG are affected largely by the launch condition of light coupled to the MMF [9]. In our experiment, the spectrum measurements are performed using a broadband LED source under the few-mode excitation condition, where an SMF is spliced to the MMF directly. Thus, the launch condition is stable and not sensitive to environment (such as vibration and fiber bending). This ensures that the set-up is flexible and stable and that the measurements are repeatable. The transmission spectra are observed with an optical spectrum analyzer (ADVANTEST Q8384) with a resolution of 0.08 nm.

Fig. 5 shows the transmission spectra of the 3° slanted MFBG at room temperature. Complex multimode couplings cause two different wavelength groups in the spectra. The short wavelength group is due to the coupling from the core modes to the cladding modes, and the long wavelength group is due to the core modes coupling to higher-order core modes [8]. When the slanted MFBG is placed in air, the bandwidth of the entire short wavelength group is about 17 nm and the separation between the transmission dips decreases from 0.56 to 0.20 nm as the wavelength increases. On the other hand, the bandwidth of the entire long wavelength group is about 5 nm, and the separation between the dips increases from 0.56 to 0.78 nm as

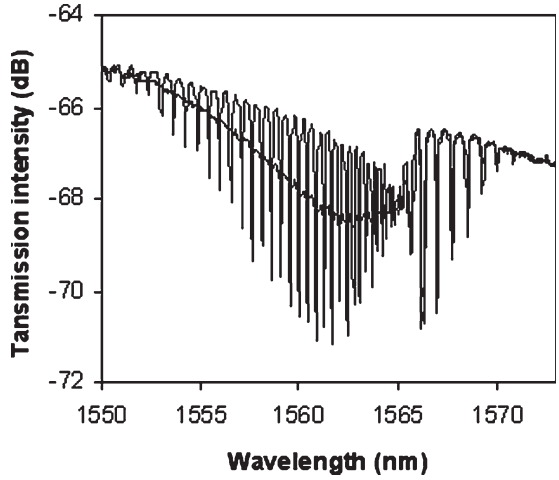

Fig. 5. Transmission spectra of the 3° slanted MFBG at room temperature thin curve: in air; heavy curve: covered with index matching oil.

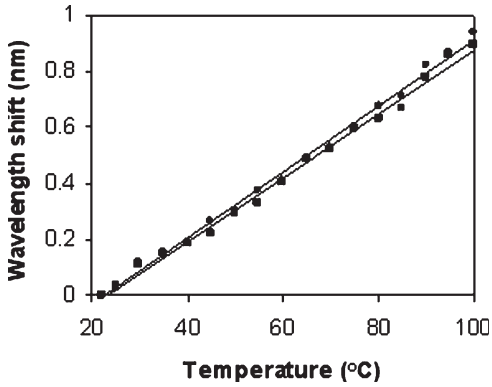

Fig. 6. Temperature dependence of wavelength shift for the $\lambda_{\mathrm{cl}}^{1}$ and the λ_{co} dips of the 3° slanted MFBG in air. The temperature sensitivities are 0.0114 and 0.0118 nm/°C, respectively.

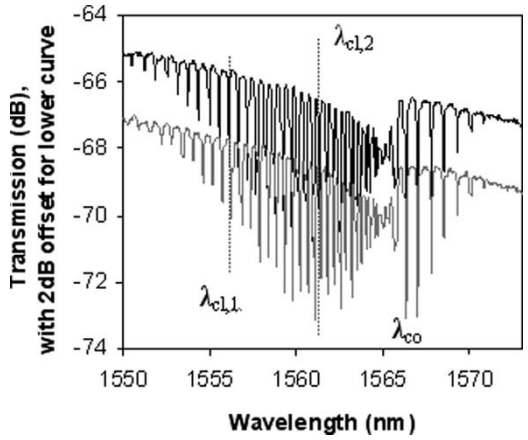

Fig. 7. Transmission spectra of the MFBG at various surroundings of refractive index value (upper curve: SRI $= 1.33$, lower curve: SRI $= 1.43$).

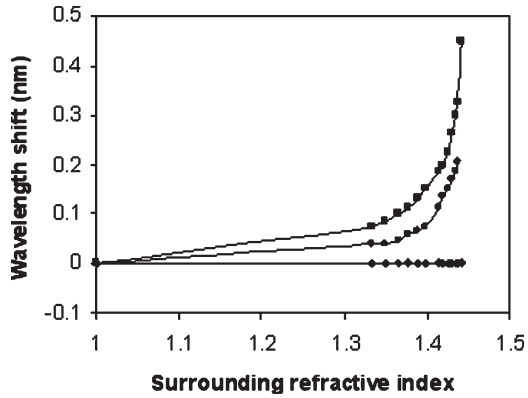

Fig. 8. Experimental measured dependence of the wavelength shift with SRI for three transmission dips. ■: $\lambda_{\mathrm{cl},1} = 1556.03$ nm; ●: $\lambda_{\mathrm{cl},2} = 1561.30$ nm; ♦: $\lambda_{\mathrm{co}} = 1566.30$ nm.

the wavelength increases. When the slanted MFBG is put into index matching oil having a refractive index of about 1.45, all the dips in the short wavelength group almost disappear since the wavelengths caused by core modes coupling to cladding modes are very sensitive to SRI, but the spectrum of the long wavelength group has no change. Here, we chose and marked two transmission dips as $\lambda_{\mathrm{cl},1}$ and $\lambda_{\mathrm{cl},2}$ in the short wavelength group and one transmission dip as λ_{co} in the long wavelength group, respectively, which are at 1556.03 nm ($\lambda_{\mathrm{cl},1}$), 1561.30 ($\lambda_{\mathrm{cl},2}$), and 1566.30 nm (λ_{co}) when SRI $= 1$ (for air). Simultaneous measurement of temperature and refractive index is achieved by testing the wavelength shifts of $\lambda_{\mathrm{cl},1}$ (or $\lambda_{\mathrm{cl},2}$) and λ_{co} dips with temperature and SRI.

The temperature dependences of $\lambda_{\mathrm{cl},1}$ and λ_{co} dips are studied by placing the slanted MFBG in a temperature chamber that is temperature controlled in the range of 22–100 °C. When the temperature rises, all the Bragg wavelengths shift linearly to longer wavelengths due to the thermal effect on the refractive index of the material and the linear expansion of the fiber. Fig. 6 shows the dependence of wavelength shift on temperature for both $\lambda_{\mathrm{cl},1}$ and λ_{co} dips in air. Both dips show linear characteristics. The temperature sensitivities ($\Delta\lambda/\Delta T$) are estimated by using linearly regression fits, which are 11.4 and 11.8 pm/°C for $\lambda_{\mathrm{cl},1}$ and λ_{co} transmission dips, respectively. The linearity of the temperature sensitivities is high and the R-squared values for $\Delta\lambda_{\mathrm{cl}}/\Delta T$ and $\Delta\lambda_{\mathrm{co}}/\Delta T$ are larger than 0.9951 within a temperature range from 22 °C to 100 °C.

The SRI dependences of $\lambda_{\mathrm{cl},1}$ (or $\lambda_{\mathrm{cl},2}$) and λ_{co} dips are studied by dipping the slanted MFBG into liquids with different refractive indices. The operation is simple and flexible since the MFBG is not sensitive to bending. Liquids with different refractive indices are obtained by mixing pure water ($n_{\mathrm{water}} = 1.33$) and glycerol ($n_{\mathrm{g}} = 1.47$) with different proportions. The measured transmission spectra of the slanted MFBG immersed in liquids having refractive indices of 1.33 and 1.43 are shown in Fig. 7. In order to show the change of spectra in two cases clearly, we add a 2-dB offset between two curves in Fig. 7. The transmission dips of the short wavelength group shift toward longer wavelengths with increasing SRI and the transmission dips become weaker since the wavelengths caused by core modes coupling to cladding modes are very sensitive to SRI because light extends more into the surrounding liquid and is lost (absorbed). In contrast, the wavelengths of the dips in the long wavelength group are unchanged because the couplings from core modes to other higher order modes are not affected by changes in the surroundings. Fig. 8 plots the wavelength shift of $\lambda_{\mathrm{cl},1}$, $\lambda_{\mathrm{cl},2}$, and λ_{co} dips with different SRIs. There is no

wavelength shift for the λ_{co} dip in the SRI range of 1–1.46 as explained above. However, the wavelength shifts of $\lambda_{\mathrm{cl},1}$ and $\lambda_{\mathrm{cl},2}$ dips become larger when SRI becomes closer to the refractive index of the fiber cladding, and the wavelength shift of $\lambda_{\mathrm{cl},1}$ is larger than that of $\lambda_{\mathrm{cl},2}$ with the same SRI change because the cladding mode corresponding to the $\lambda_{\mathrm{cl},1}$ dip is a higher mode $(\mathrm{HE}_{1,14})$ and is affected more strongly by the surrounding medium. The theoretical and experimental values for the wavelength shifts of transmission dips with SRI are in good agreement as the comparison of Figs. 4 and 8 reveals. In the simulation, we have assumed the index of the core to be constant whereas the core actually is a graded index, and this does not affect the good agreement between experimental and theoretical results because Figs. 4 and 8 are influenced primarily by the index of the cladding and SRI. The measured range of SRI is between 1 and 1.45 because both $\lambda_{\mathrm{cl},1}$ and $\lambda_{\mathrm{cl},2}$ dips virtually disappear when SRI increases to 1.45. This is the same effect as shown in Fig. 5 when the fiber is immersed in index matching oil.

The mechanism by which we can simultaneously measure temperature and SRI is as follows. The wavelength shift of the λ_{co} dip (coupling from one core mode to other core mode) is caused only by the change in temperature, meaning that the temperature can be measured only from the wavelength shift of the λ_{co} dip. The wavelength shift of the $\lambda_{\mathrm{cl},1}$ dip (coupling from one core mode to one cladding mode) is contributed by both the thermal effect and the SRI. In order to get a net effect due to the SRI, the temperature-induced wavelength shift needs to be subtracted from the total wavelength shift of the $\lambda_{\mathrm{cl},1}$ dip by use of the temperature information measured from the λ_{co} dip. Thus, the simultaneous temperature and SRI measurement is achieved by testing the wavelength shifts of the $\lambda_{\mathrm{cl},1}$ and λ_{co} dips of the slanted MFBG.

IV. Conclusion

In conclusion, we observed the properties of a 3° slanted MFBG, in which two different wavelength groups appear in the transmission spectra. The transmission dips, which are due to the coupling from one core mode to cladding modes, are sensitive to both SRI and the temperature, whereas the dips due to coupling from one core mode to other core modes are sensitive to temperature only. The simultaneous measurement of temperature and refractive index was achieved by measuring the wavelength shifts of two transmission dips in different wavelength groups of the slanted MFBG. The sensor based on the MFBG is simple and compact because, for a practical measurement, the MFBG is stable and insensitive to bending. Furthermore, it provides better resolution. All these advantages make it preferable to sensors based on LPGs.

References

[1] H. J. Patric, A. D. Kersey, and F. Bucholtz, "Analysis of the response of long period fiber gratings to external index of refraction," *J. Lightw. Technol.*, vol. 16, no. 9, pp. 1606–1612, Sep. 1998.

[2] M. N. Ng, Z. Chen, and K. S. Chiang, "Temperature compensation of long-period fiber grating for refractive-index sensing with bending effect," *IEEE Photon. Technol. Lett.*, vol. 14, no. 3, pp. 361–362, Mar. 2002.

[3] B. A. L. Gwandu, X. Shu, T. D. P. Allsop, W. Zhang, L. Zhang, and I. Bennion, "Simultaneous refractive index and temperature measurement using cascaded long-period grating in double-cladding fiber," *Electron. Lett.*, vol. 38, no. 14, pp. 695–696, Jul. 2002.

[4] X. Shu, B. A. L. Gwandu, Y. Liu, L. Zhang, and I. Bennion, "Sampled fiber Bragg grating for simultaneous refractive index and temperature measurement," *Opt. Lett.*, vol. 26, no. 11, pp. 774–776, Jun. 2001.

[5] Y.-G. Han, B. H. Lee, W.-T. Han, U.-C. Paek, and Y. Chung, "Fiber-optic sensing applications of a pair of long-period fiber gratings," *Meas. Sci. Technol.*, vol. 12, no. 7, pp. 778–781, Jul. 2001.

[6] K. Schroeder, W. Ecke, R. Mueller, R. Willsch, and A. Andreev, "A fiber Bragg grating refractometer," *Meas. Sci. Technol.*, vol. 12, no. 7, pp. 757–764, Jul. 2001.

[7] G. Laffont and P. Ferdinand, "Tilted short-period fiber-Bragg-grating induced coupling to cladding modes for accurate refractometry," *Meas. Sci. Technol.*, vol. 12, no. 7, pp. 765–770, Jul. 2001.

[8] X. Yang, C. Zhao, J. Zhou, X. Guo, J. Ng, X. Zhou, and C. Lu, "The characteristics of fiber slanted gratings in multimode fiber," *Opt. Commun.*, vol. 229, no. 1–6, pp. 161–165, Jan. 2004.

[9] T. Mizunami, T. V. Djambova, T. Niiho, and S. Gupta, "Bragg gratings in multimode and few-mode optical fibers," *J. Lightw. Technol.*, vol. 18, no. 2, pp. 230–235, Feb. 2000.

[10] K. Kitayama, S. Seikai, and N. Uchida, "Impulse response prediction based on experimental mode coupling coefficient in a 10-km long graded-index fiber," *IEEE J. Quantum Electron.*, vol. QE-16, no. 3, pp. 356–362, Mar. 1980.

[11] D. Marcuse, *Light Transmission Optics*, 2nd ed. New York: Van Nostrand, 1982.

[12] J. H. Povlsen, P. Danielsen, and G. Jacobsen, "Modal propagation constants, group delays, and eigenfields for practical multimode graded-index fibers," *J. Opt. Soc. Amer.*, vol. 72, no. 11, pp. 1506–1513, Nov. 1982.

[13] Y. Liu, B. M. A. Rahman, Y. N. Ning, and K. T. V. Grattan, "Accurate mode characterization of graded-index multimode fibers for application on mode-noise analysis," *Appl. Opt.*, vol. 34, no. 9, pp. 1540–1543, Mar. 1995.

[14] T. Erdogan, "Cladding-mode resonances in short- and long-period fiber grating filters," *J. Opt. Soc. Amer. A, Opt. Image Sci.*, vol. 14, no. 8, pp. 1760–1773, Aug. 1997.

[15] C. Tsao, *Optical Fiber Waveguide Analysis*. New York: Oxford Univ. Press, 1992.

Chun-Liu Zhao received the Ph.D. degree in optics from the Nankai University, Tianjin, China, in 2002.

From 2002 to 2004, she was a Research Fellow at the Lightwave Department, Institute for Infocomm Research, Singapore. Since 2004, she has been a Postdoctoral Fellow at the Electrical Engineering Department, Hong Kong Polytechnic University, Hong Kong. Her research interests include fiber grating, optical fiber amplifiers and lasers, and applications based on photonic crystal fibers.

Xiufeng Yang, photograph and biography not available at the time of publication.

M. S. Demokan (SM'89), photograph and biography not available at the time of publication.

W. Jin (M'95–SM'98), photograph and biography not available at the time of publication.